Monatshefte für Chemie 130, 283–293 (1999)

Monatshefte für Chemie
Chemical Monthly
© Springer-Verlag 1999
Printed in Austria

Protonation and Coordinative Properties of 14-Membered Tetraaza Macrocycles Linked to Phthalocyanines

Ulvi Avciata[1], Abdürrezak E. Bozdoğan[1], Makbule Koçak[2], Ahmet Gül[2], Ali Ihsan Okur[2], and **Özer Bekaroğlu[2,*]**

[1] Department of Chemistry, Yıldız Technical University, TR-80270 Şişli, Istanbul, Turkey
[2] Department of Chemistry, Technical University of Istanbul, TR-80626 Maslak, Istanbul, Turkey

Summary. The protonation behaviour and coordination ability of 14-membered tetraaza macrocycles in the periphery of a phthalocyanine core (*L*) together with a model compound of identical macrocyclic structure towards Co^{2+}, Ni^{2+}, and Cu^{2+} has been studied potentiometrically at 25°C in 0.3 *M* KCl solution. The protonation pattern of *L* indicates that the basicities of three secondary amino groups are high and comparable; the fourth one is of rather low basicity, probably due to the effect of charge repulsion. It is shown that the potentiometric data for the phthalocyanine derivative can be used to estimate the stability constants and the distribution diagram for the species in solution by treating each macrocycle *L′* at the periphery of the phthalocyanine core separately using the program TITFIT.

Keywords: Phthalocyanine; Tetraaza macrocycles; Stability constants.

Protonierung und koordinative Eigenschaften von 14-gliedrigen Tetraazamakrocyclen an der Peripherie von Phthalocyaninen

Zusammenfassung. Protonierungsverhalten und Koordinationsfähigheit von vierzehngliedrigen Tetraazamacrocyclen an der Peripherie eines Phthalocyanins (*L*) sowie einer Modellverbindung mit gleicher makrocyclischer Struktur wurde in 0.3 *M* KCl-Lösung für Co^{2+}, Ni^{2+} und Cu^{2+} potentiometrisch bestimmt. Das Protonierungsverhalten von *L* zeigt, daß die Basizität von drei sekundären Aminogruppen hoch und vergleichbar, die der vierten, wahrscheinlich bedingt durch gegenseitige Abstoßung der Ladungen, jedoch ziemlich schwach ist. Die Stabilitätskonstanten können aus den potentiometrischen Daten bestimmt werden. Für die jeweiligen macrocyklischen Liganden *L′* an der Peripherie des Phthalocyanins wurden die Stabilitätskonstanten und das Verteilungsdiagramm für die Spezies in Lösung mit Hilfe des TITFIT-Programms bestimmt.

Introduction

The interaction of various macrocyclic ligands with metal ions has been of considerable current interest during the last three decades [1, 2]; in this context,

* Corresponding author

stepwise variations of the ring size [3], nature of donor groups [4], and the rigidity of the macrocycles [5] have been studied in detail with respect to different metal ions. Completely saturated tetraaza macrocycles (*i.e.* cyclams) and their derivatives with fused aromatic rings have been proven to be especially useful to obtain selective complexation sites for various transition metal ions [6]. The flexibility of the ligand is closely related to the degree of unsaturation and the number of fused rings. An important point in all these macrocyclic cyclam derivatives is the presence of only one macrocycle capable of binding metal ions; interactions between metal ions and more than one macrocyclic donor on the same molecule have not been treated so far.

During the last decade we have reported a number of phthalocyanines, the molecular structures of which may be thought of as a phthalocyanine core with four peripherally fused macrocyclic rings [7]. The macrocyclic groups have been crown ethers [8, 9], monoaza crown ethers [10], tetraaza [11], diazatrioxa [12], diazadioxa [13], or tetrathia macrocycles [14]. These structures allow for the chelation of a wide range of metal ions at the periphery in addition to that at the inner core; pentanuclear complexes with alkali and earth alkali cations, transition metals, and/or rare earth metal ions are formed [15]. The alkali picrate extraction from aqueous to organic phase has been proven to be a practical way of determining the order of interaction between alkali metal ions and crown ether substituents [8].

In the present paper, the interaction of transition metal ions with four tetraazamacrocycles present as peripheral substituents of a phthalocyanine core was investigated by potentiometric titration. A comparative study with a 14-membered analogus tetraaza compound as a model was carried out simultaneously.

Results and Discussion

The synthesis of 2,5,8,11-*tetrakis*-(*p*-tolylsulfonyl)-1,2,3,4,5,6,7,9,10,11,12-dodecahydrobenzo[1][1,4,7,10]tetraazacyclotetradecine as its 14,15-dibromo derivative and the Cu(II) phthalocyanine derived from it was accomplished as described previously [11, 16]. The detosylated derivatives of these two compounds, denoted as *L* and *Pc*, were used as ligands in the present work (Fig. 1). A comparison of these two structures indicates that the *Pc* containing four tetraazamacrocycle units on the periphery is equivalent to four *L* units held together by the phthalocyanine core; it is therefore practical to take a quarter of the *Pc* molecule as L' (the part highlighted with dashed lines in Fig. 1) when comparing complexation properties.

The protonation behaviour of *L* and *Pc* was studied in 0.3 *M* KCl solution at 298 K; the corresponding, data are presented in Table 1 and Figs. 2–10. A maximum number of four protons can be liberated from the ligand *L* in the protonated form upon titration with a strong base in the *pH* range of 2.0–12.0. The first three protonation constants of *L* are high and of the same order, whereas the fourth one is somewhat lower. A similar effect observed in the last protonation step of an open chain tetramine, *i.e.* 4,7-diaza-1,10-diaminodecane, in which a symmetrical arrangement of two propylenic and one ethylenic chains are present between the nitrogens [17]. In the case of macrocycle *L*, there are three ethylenic chains between the aza functions; the fourth one is a C_4 unit which permits sufficient separation of the protonated aza groups. Therefore, the basicities of *L* and

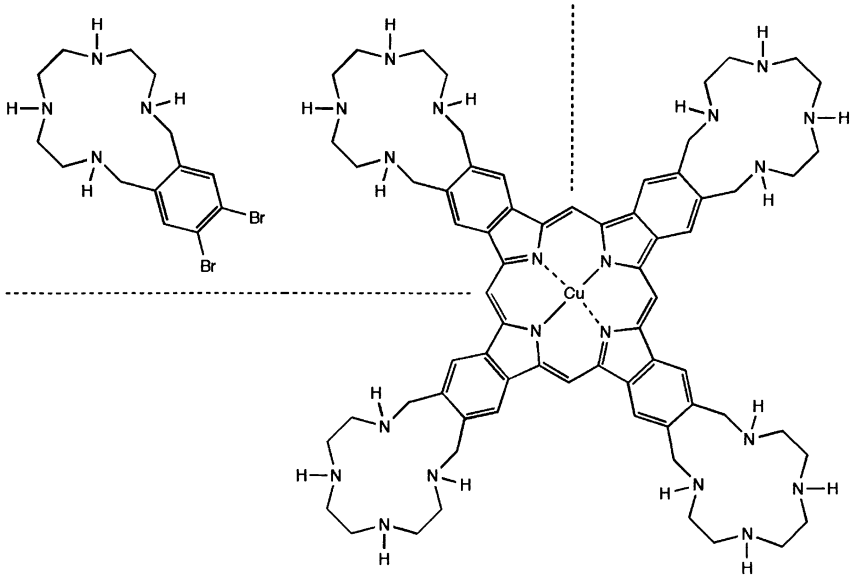

Fig. 1. Structure of L and Pc; the part highlighted with dashed lines corresponds to L'

Table 1. Protonation and overall formation constants of L and L' at 25°C; $I = 0.30\,M$ KCl, $T_M = 0.001\,M$, $T_L = 0.001\,M$, $T_{L'} = 0.001\,M$; $\log\beta$: mean value of two determinations; Δ: standard deviation

Metal ion	Species	$\log\beta$	Δ	Species	$\log\beta$	Δ
	HL	9.99	0.04	HL'	10.18	0.04
H^+	H_2L	19.99	0.02	H_2L'	20.28	0.07
	H_3L	29.99	0.04	H_3L'	29.50	0.06
	H_4L	37.00	0.04	H_4L'	35.39	0.08
	CuL	9.50	0.03	CuL'	12.54	0.05
Cu^{2+}	CuHL	22.46	0.05	CuHL'	20.34	0.08
	CuH_2L	31.95	0.04	CuH_2L'	32.17	0.12
	CuH_3L	38.48	0.06	CuH_3L'	37.90	0.09
	NiL	9.45	0.06	NiL'	13.80	0.05
Ni^{2+}	NiHL	21.46	0.08	NiHL'	21.86	0.07
	NiH_2L	32.29	0.06	NiH_2L'	31.14	0.06
	NiH_3L	38.09	0.06	NiH_3L'	38.89	0.07
	NiL(OH)	−3.5	0.08			
	CoL	17.51	0.08	CoL'	15.76	0.03
Co^{2+}	CoHL	23.97	0.06	CoHL'	25.39	0.06
	CoL(OH)	9.31	0.09	CoH_2L'	34.01	0.09
	Co$L(OH)_2$	0.60	0.07	CoH_3L	40.46	0.12
				CoL'(OH)	5.49	0.12
				Co$L'(OH)_2$	−4.86	0.15

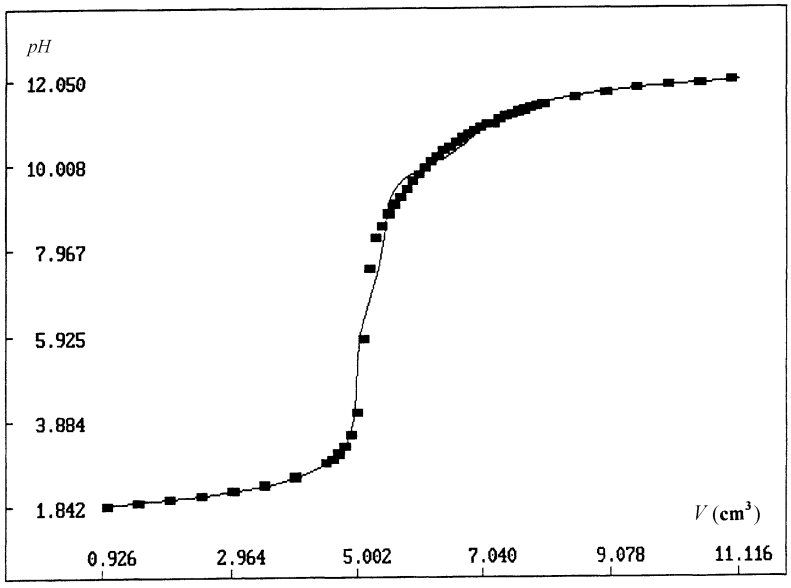

Fig. 2. Titration curve of L with 0.1 M NaOH

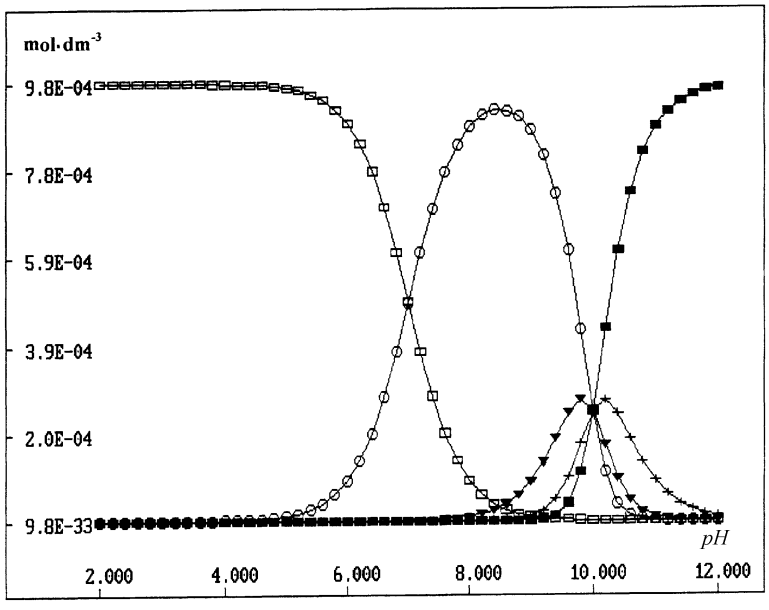

Fig. 3. Typical distribution diagrams for L (□□□: $[H_4L]^{4+}$, ooo: $[H_3L]^{3+}$, ▼▼▼: $[H_2L]^{2+}$, +++: $[HL]^{+}$, ■■■: L)

the open-chain analog are similar. The distribution diagram of L in Fig. 3 indicates that the fully protonated species of L, $[H_4L]^{4+}$, predominates at $pH = 5$, and $[H_3L]^{3+}$ shows a maximum around $pH = 8.5$. Doubly and monoprotonated species appear around $pH = 10$ at relatively low concentrations, and the free ligand L appears to dominate above $pH = 11$. The high positive charge on L around neutral

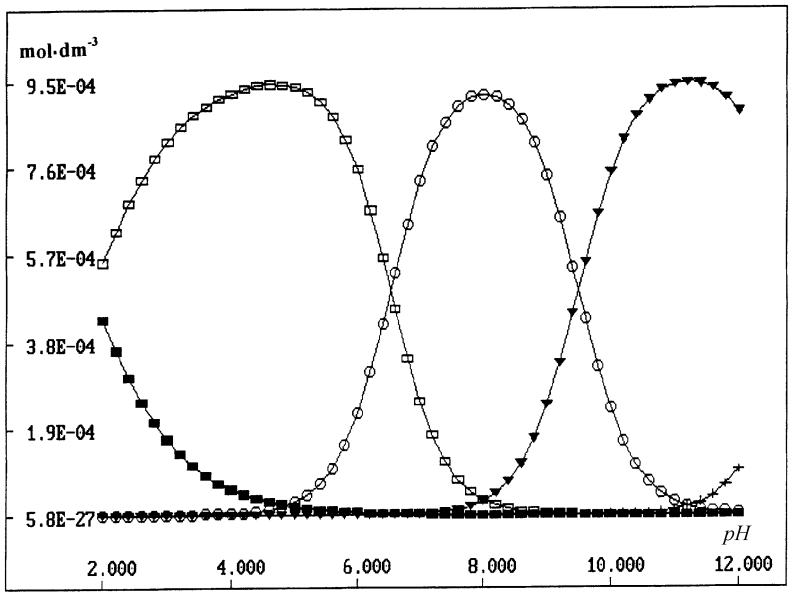

Fig. 4. Typical distribution diagrams for the Cu^{2+}-*L* system (■■■: Cu^{2+}, +++: $[CuL]^{2+}$, ▼▼▼: $[CuHL]^{3+}$, ooo: $[CuH_2L]^{4+}$, □□□: $[CuH_3L]^{5+}$)

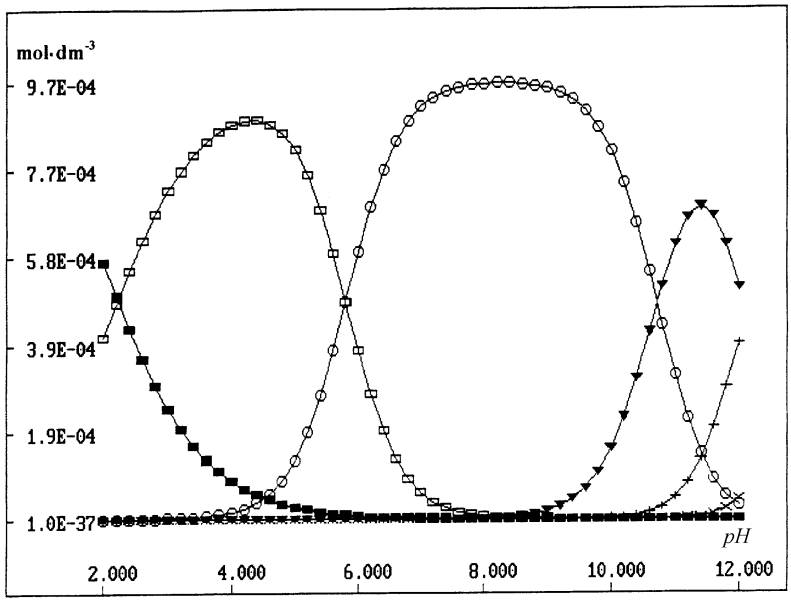

Fig. 5. Typical distribution diagrams for the Ni^{2+}-*L* system (■■■: Ni^{2+}, +++: $[NiL]^{2+}$, ▼▼▼: $[NiHL]^{3+}$, ooo: $[NiH_2L]^{4+}$, □□□: $[NiH_3L]^{5+}$, xxx: $[NiL(OH)]^{+}$)

pH makes this ligand a promising potential receptor for anionic species [18]; this aspect will be dealt with in further studies.

In the case of the phthalocyanine derivative, all sixteen aza groups present on the peripheral substituents of *Pc* should be taken into account separately as

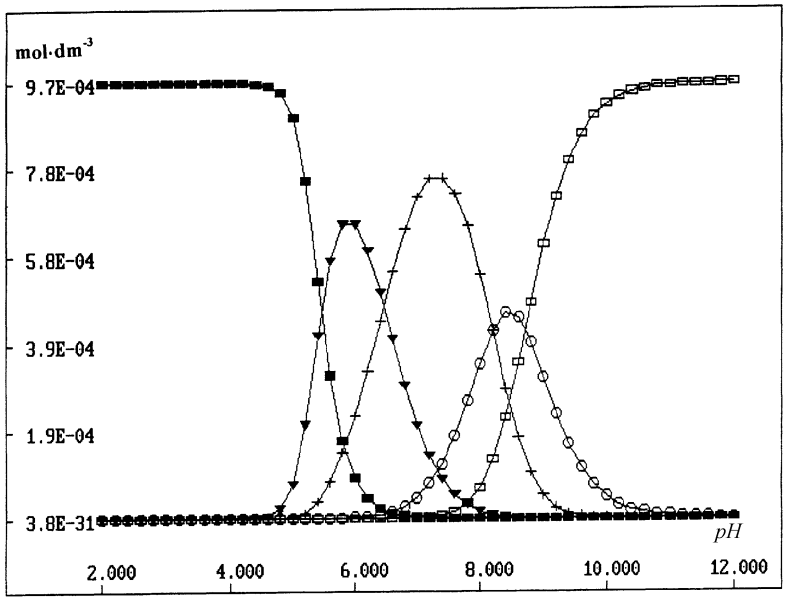

Fig. 6. Typical distribution diagrams for the Co^{2+}-L system (■■■: Co^{2+}, +++: $[CoL]^{2+}$, ▼▼▼: $[CoHL]^{3+}$, ooo: $[CoL(OH)]^{+}$, □□□: $[CoL(OH)_2]$)

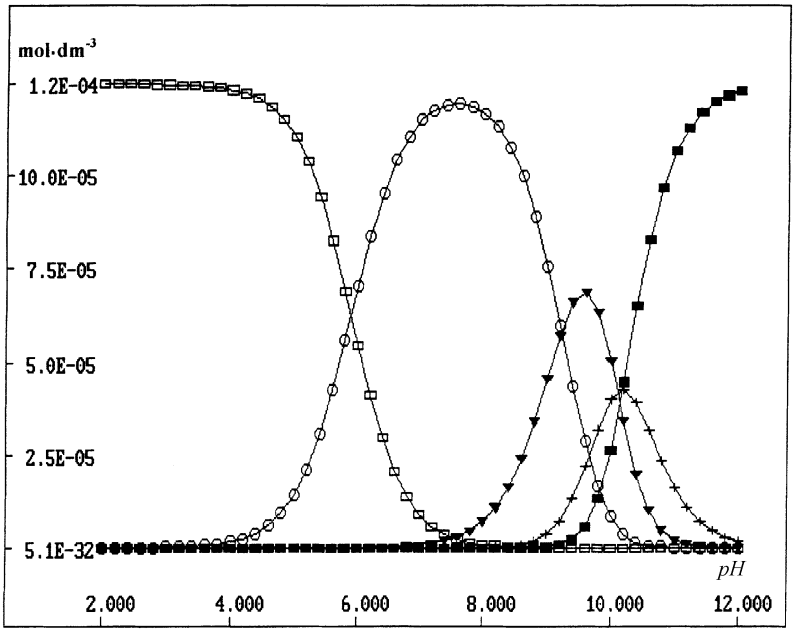

Fig. 7. Typical distribution diagrams for L' (□□□: $[H_4L']^{4+}$, ooo: $[H_3L']^{3+}$, ▼▼▼: $[H_2L']^{2+}$, +++: $[HL']^{+}$, ■■■: L')

protonation sites. However, it is not possible to obtain reliable results for all 16 protonation steps using the present mathematical models. Indeed, the number of variables will be at least doubled when only mononuclear complexes are included. A practical solution to this problem can be reached taking into account the

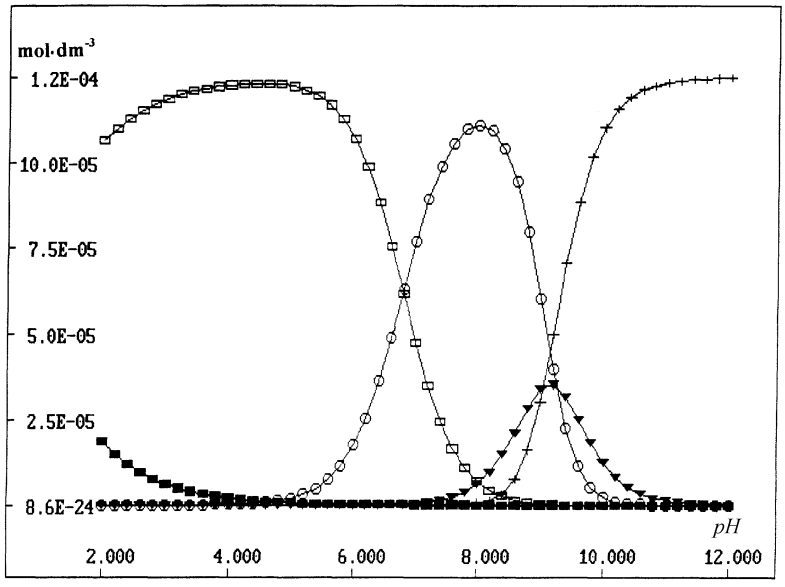

Fig. 8. Typical distribution diagrams for the Cu^{2+}-L' system (■■■: Cu^{2+}, +++: $[CuL']^{2+}$, ▼▼▼: $[CuHL']^{3+}$, ooo: $[CuH_2L']^{4+}$, □□□: $[CuH_3L']^{5+}$)

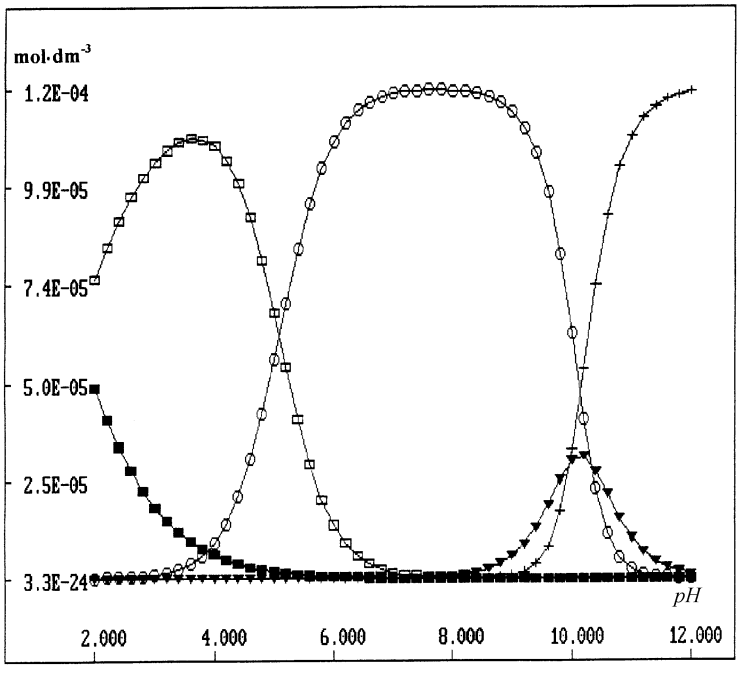

Fig. 9. Typical distribution diagrams for the Ni^{2+}-L' system (■■■: Ni^{2+}, +++: $[NiL']^{2+}$, ▼▼▼: $[NiHL']^{3+}$, ooo: $[NiH_2L']^{4+}$, □□□: $[NiH_3L']^{5+}$)

symmetrical distribution of tetraaza macrocycles around the phthalocyanine core and their sufficiently isolated positions which allows individual calculation for each macrocycle separately. Consequently, the number of protonation steps was 4 both for L and L', the latter corresponding to a single tetraaza macrocycle (Fig. 1),

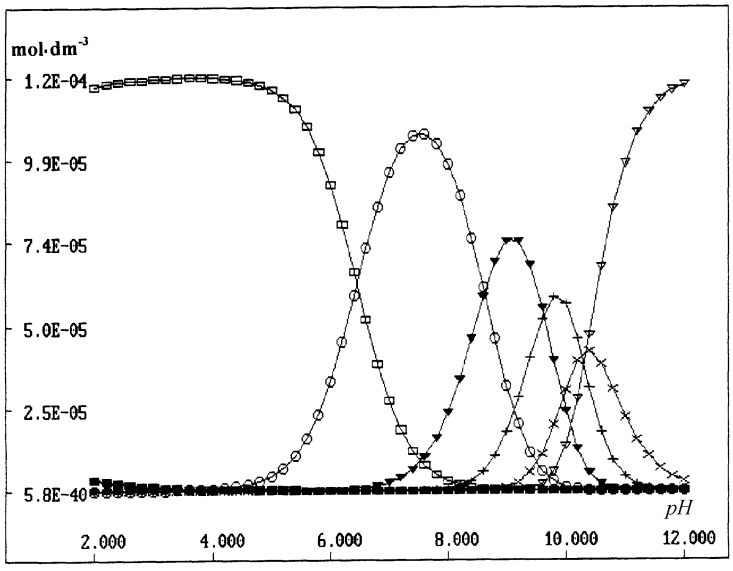

Fig. 10. Typical distribution diagrams for the Co^{2+}-L' system (■■■: Co^{2+}, +++: $[CoL']^{2+}$, ▼▼▼: $[CoHL']^{3+}$, ooo: $[CoH_2L]^{4+}$, □□□ $[CoH_3L']^{5+}$, xxx: $[CoL'(OH)]^{+}$, ▽▽▽: $[CoL'(OH)_2]$)

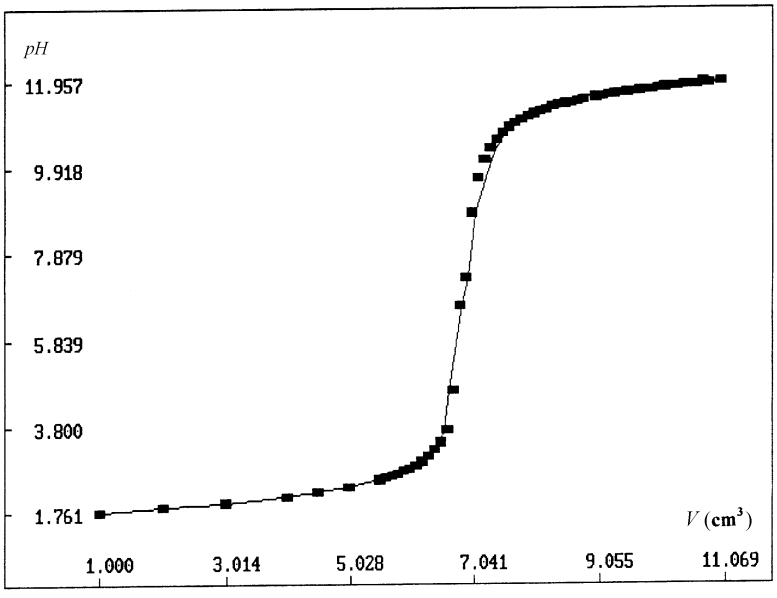

Fig. 11. Titration curve of the Cu^{2+}-L system with 0.1 M NaOH

and the theoretical calculations closely follow the experimental values. From the four protonation constants listed in Table 1, three are of about the same magnitude; only the last one is somewhat lower. This can be taken as a clear indication that all dialkylaza functions on the macrocycles have the same chemical environments, and

the effect of charge accumulation induced by the cyclic topology is effective only for binding the last proton of each macrocycle.

In Table 1 we also report the stability constants for the formation of mononuclear complexes for each tetraaza macrocycle in the case of both L and L' with the divalent first row metal ions Cu^{2+}, Ni^{2-}, and Co^{2+}. The magnitude of the stability constants for the formation of the non-protonated species $(ML)^{2+}$ follows the order $Co^{2+} \gg Cu^{2+} > Ni^{2+}$ for L and $Co^{2+} > Ni^{2+} \geq Cu^{2+}$ for L'. The number of protonated complexes and the values for the stepwise protonation constants of $[ML]^{2+}$ give some indication of the coordination numbers of different metal ions. Whereas $[CuL]^{2+}$ and $[NiL]^{2+}$ appear to be capable of protonation up to $[MLH_3]^{5+}$ and the values of the logarithms of the stepwise protonation constants are higher than those corresponding to the protonation of amine, $[CoL]^{2+}$ forms only the mono-protonated species $[CoLH]^{3+}$. However, mono- and dihydroxo complexes of cobalt(II) can be observed at reasonably high pH values.

Titration data were processed by the TITFIT program to obtain formation curves and the distribution of each complex *vs.* pH at various concentrations of ligand and metal ion [19, 20]. The validity of the models is verified by the excellent matching of the experimental and calculated potentiometric data. The refinement converged satisfactorily when the protonated and hydroxo complexes listed in Table 1 are taken into account. In the case of ligand L, it should be pointed out that in addition to $[ML]^{2+}$ there are three protonated complexes for Cu^{2+}, three protonated and one hydroxo complex for Ni^{2+}, and one protonated and two hydroxo complexes for Co^{2+}. Potentiometric curves of protonated ligand alone and in the presence of Cu^{2+} are given to illustrate the changes between these two cases (Fig. 2 and Fig. 11). The relative importance of the various species in each pH range is shown by the distribution diagrams for L and L' with Co^{2+}, Ni^{2+}, and Cu^{2+} (Figs. 4–6 and 8–10). Some general observations can be made concerning the complexation behaviour of these two ligands with the cited metal ions. In the case of the Co-L system, complexation starts at low pH values (*ca.* $pH = 5.0$) with the formation of $[CoLH]^{3+}$ corresponding to the displacement of three protons; the maximum fraction of this complex is 62% at $pH = 5.85$. The initial reaction with Ni^{2+} begins at even lower pH values (*ca.* $pH = 3.0$) corresponding to the displacement of one proton; the maximum conversion to this fraction (84%) occurs at $pH = 4.0$. When the pH reaches 8.0, the complex $[NiLH_2]^{4+}$ is the only species, its maximum fraction being about 99%. NiL(OH) appears at very high pH values (near 12).

When similar distribution diagrams are produced for each macrocycle L' on the *Pc* core, general trends follow those encountered for L. Free unprotonated L' is appearing above $pH = 10$, and it becomes the only species around $pH = 12$. Potentiometric titrations in the presence of Cu^{2+} ions can be interpreted by, assuming the presence of mainly triply protonated compounds up to $pH = 6$ doubly protonated ones up to 10, and $[ML']^{2+}$ afterwards. The titration curve for the Co^{2+}-L' system closely fits a diagram in which all steps of triply protonated to unprotonated complexes are formed up to $pH = 10$, and mono- and dihydroxo derivatives are successors. The interaction of L' and Ni^{2+} shows a pattern similar to that of Cu^{2+}, but the unprotonated complex $[ML']^{2+}$ is dominant at $pH > 9$. As a conclusion, it should be pointed out that when the macrocyclic coordination sites

are bridged with sufficiently inert cores such as phthalocyanines, each donor group can be considered separately for complexation.

Experimental

The N-tosylated tetraazamacrocyclic ligand was synthesized as its dibromo derivative as described previously [11]. It detosylation to *L* was accomplished by refluxing in HOAc+HBr (48%) for 48 h. The synthesis and purity of the phthalocyanine has also been reported [11, 16] (Fig. 1). The concentrations of stock solutions of metal ions were determined by atomic absorption spectrometry.

Potentiometric measurements

Potentiometric titrations were carried out using a Metrohm E-415 dosimate and a Metrohm E-510 *pH* meter. A Metrohm 6.0204.000 combined glass electrode was used for *pH* and *emf* measurements. The microelectrode was standardized from calculated acid concentrations in titrations covering the *pH* range from 2.0 to 12.0. The ionic strength was kept constant at 0.3 *M* KCl. All titration solutions were prepared in a total volume of 40.0 ml thermostatted at 25±0.1°C.

The following solutions were prepared to obtain the titration curves:

solution A: $HClO_4$ (2.5 ml, 0.1 *M*), KCl (15 ml, 0.3 *M*), water (22.5 ml);

solution B: $HClO_4$ (2.5 ml, 0.1 *M*), KCl (15 ml, 0.3 *M*), solution of *L* or *L*′ in ethanol (2.5 ml, 0.01 *M*), water (20 ml);

solution C–F: $HClO_4$ (2.5 ml, 0.1 *M*), KCl (15 ml, 0.3 *M*), solution of *L* or *L*′ in ethanol (2.5 ml, 0.01 *M*), aqueous solution of metal salt (*i.e.* $CuCl_2 \cdot 2H_2O$, $NiCl_2 \cdot 6H_2O$, $CoCl_2 \cdot 6H_2O$, $UO_2(AcO)_2 \cdot 4\ H_2O$; 2.5 ml, 0.01 *M*), water (17.5 ml).

The solutions were titrated with 0.1 *M* NaOH in increments of 0.2 ml under an atmosphere of N_2. The corresponding change in the *pH* value of the solution was measured. Three separate titrations were performed for each particular ligand-metal combination, and data were analyzed by the program TITFIT [19, 20]. The results are summarized in Table 1 and Figs. 2–10.

References

[1] Dietrich B, Viont P, Lehn JM (1992) Macrocyclic Chemistry. VCH, Weinheim
[2] Vögtle F (1991) Supramolecular Chemistry – An Introduction. Wiley, Chichester
[3] Thöm VJ, Hancock RD (1985) J Chem Soc Dalton Trans 1877
[4] Cabral MF, Delgado R (1994) Helv Chim Acta **77**: 515
[5] Costa J, Delgado R (1993) Inorg Chem **32**: 5257
[6] Gül A, Okur AI, Cihan A, Tan N, Bekaroğlu Ö (1986) J Chem Research 90
[7] Bekaroğlu Ö (1996) Appl Organometal Chem **10**: 605
[8] Koray AR, Ahsen V, Bekaroğlu Ö (1986) J Chem Soc Chem Commun 932; Ahsen V, Yılmazer E, Ertas M, Bekaroğlu Ö (1988) J Chem Soc Dalton Trans 401
[9] Okur AI, Gül A, Cihan A, Tan N, Bekaroğlu Ö (1990) Synth React Inorg Met Org Chem **20**: 1399; Sarıgül S., Bekaroğlu Ö (1989) Chem Ber **122**: 291
[10] Musluoğlu E, Ahsen V, Gül A, Bekaroğlu Ö (1991) Chem Ber **124**: 2531
[11] Koçak M, Cihan A, Okur AI, Bekaroğlu Ö (1991) J Chem Commun 577; Ahsen V, Gül A, Bekaroğlu Ö (1991) J Chem Soc Dalton Trans 3367
[12] Gümüs G, Öztürk Z, Ahsen V, Gül A, Bekaroğlu Ö (1992) J Chem Soc Dalton Trans 2485
[13] Hamuryudan E, Bekaroğlu Ö (1993) J Chem Res (S) 460
[14] Gürek A, Bekaroğlu Ö (1994) Helv Chim Acta **77**: 1616
[15] Koçak M, Okur AI, Bekaroğlu Ö (1994) J Chem Soc Dalton Trans 323
[16] Koçak M, Gürek A, Gül A, Bekaroğlu Ö (1994) Chem Ber **127**: 355

[17] Aguilar JA, Bianchi A, Garcia-Espana E, Luis SV, Llinanes JM, Ramirez JA, Soriano C (1994) J Chem Soc Dalton Trans 637
[18] Hancock RD, Martell AE (1989) Chem Rev **89**: 1875
[19] Zuberbühler AD, Kaden TA (1982) Talanta **29**: 201
[20] Avcıata U, Bozdoğan AE, Koçak M, Gül A, Bekaroğlu Ö (1995) J Coord Chem **35**: 319

Received April 6, 1998. Accepted (revised) June 5, 1998